Spontaneous emission from Λ-type three-level atom driven by bichromatic field in anisotropic double-band photonic crystals

Kai Ling(凌凯)[1], Li Jiang(姜丽)[1,†], Ren-Gang Wan(万仁刚)[2,‡], and Zhi-Hai Yao(姚治海)[1]

[1] *Changchun University of Science and Technology, Changchun* 130000, *China*
[2] *School of Physics and Information Technology, Shaanxi Normal University, Xi'an* 710062, *China*

(Received 30 August 2022; revised manuscript received 15 November 2022; accepted manuscript online 17 November 2022)

The spontaneous emission property of Λ-type three-level atom driven by the bichromatic field in the anisotropic double-band photonic crystal is calculated by *n*-times iteration method. The influence of different parameters on atomic spontaneous emission is studied, and the phenomena of atomic spontaneous emission are explained in the dressed state representation. It is found that the spontaneous emission spectra of the atom driven by the bichromatic field presents a multi-peak comb structure. The position of the emission peak is determined by the initial state of the atom, and the interval between the neighboring emission peaks is the detuning δ of the bichromatic field. When the ratio between Rabi frequency intensity and the detuning δ of the bichromatic field remains unchanged, the intensity of each emitted peak remains invariant. The spontaneously emitted peak can be annihilated in the band gap and enhanced near the band edge in the anisotropic photonic crystals. Meanwhile, we also observe the fluorescence quenching phenomenon in the spontaneous emission spectra. The research in this paper provides the theoretical guidance for the control of atomic spontaneous emission.

Keywords: photonic crystal, bichromatic field, spontaneous emission spectra, dressed state

PACS: 42.70.Qs, 32.80.Qk, 42.50.Gy **DOI:** 10.1088/1674-1056/aca39b

1. Introduction

Spontaneous emission is the basic process of the interaction between light and matter. The control of the atomic spontaneous emission is an important topic in quantum optics, which is of great significance in nonlinear optics and laser physics.[1] It has a wide range of applications, such as the entanglement control,[2] atomic high-precision localization[3,4] and spectroscopy,[5] quantum information and computing.[6] There are two ways to control the spontaneous emission in the present work: one is to add a driving field coupling between the two levels in the atom, and the other is to change the environment in which the atom is located.

A Lorentz-line peak was formed when the two-energy atom in vacuum spontaneously emitted from the upper level to the lower level.[7] When the two-level atom was driven by a strong monochromatic field, a two-peak structure called the Autler–Townes spectrum occurred.[8] When the two-upper level was coupled by the coherent field in the three-level atom, dark lines appeared in the spontaneous emission spectrum due to quantum interference effect.[9] When the three-level atom was coupled by a microwave field, the narrow spectral lines appeared in the spontaneous emission spectrum.[10] In the multi-level atom coupled by an external field, the multi-peak structure as well as multiple fluorescence quenching points were observed in the spontaneous emission spectrum.[11] There were more interesting quantum phenomena in the atom coupled by bichromatic excitation or polychromatic excitation. It was found that the argon atoms coupled with bichromatic fields could produce semi-integer high-order harmonic emissions.[12] The detuning and Rabi frequency of the bichromatic field could be used to realize the localization of three-dimensional Rydberg atoms.[13] Hu *et al.* studied the spontaneous emission phenomenon of Λ-type three-level atom coupled by the trichromatic field with the method of density matrix equation and quantum regression theorem.[14] It was found that the emission spectrum was depended on the phase difference of the trichromatic field, and the spectral line selective cancellation could be achieved by changing the amplitude and phase of the trichromatic field. Meanwhile, Hu studied the spontaneous emission spectrum of Ξ-type three-level atom driven by two bichromatic fields.[15] They found that the selective elimination and complete elimination of the fluorescence spectrum were achieved by changing the phase difference of the bichromatic fields. The emission and absorption of the atom were a pair of reciprocal processes, and the splitting effect of spectral peaks occurred in both emission and absorption spectra of Ξ-type three-level atom by adjusting the relative phase of the bichromatic fields.[16] To our knowledge, the use of polychromatic excitation was an effective way to control the atomic multi-peaked spontaneous emission.

Photonic crystal[17] is a kind of material with periodic di-

†Corresponding author. E-mail: jiangli@cust.edu.cn
‡Corresponding author. E-mail: wrg@snnu.edu.cn

© 2023 Chinese Physical Society and IOP Publishing Ltd

electric structure. When the frequency of the light is within the photonic band gap, it can not pass through the photonic crystal. And the density of states (DOS) at the edge of the photonic band gap is different from that of vacuum. Therefore, photonic crystal can be used to control the atomic spontaneous emission. The spontaneous emission of a two-level atom in the anisotropic photonic crystal was studied by Yang *et al.*,[18,19] and it was found that the population on the atom showed the oscillation behavior. Zhang *et al.* studied the regulation of the spontaneous emission process of the two-level atom in the excited state using the dynamic environmental library.[20] The results showed the system coherence evolution was protected. Huang *et al.* observed the spontaneous emission spectra of the Λ-type three-level atom in anisotropic photonic crystal.[21] They found that the center and intensity of the radiation spectrum could be obviously controlled by adjusting system parameters. Zhang *et al.* found that the density of states of photonic crystal determined the relative height of the middle peak in the spontaneous emission spectrum of Λ-type and V-type three-level atoms.[22] It made a two-peak structure with wide dark lines appearing in the spontaneous emission spectrum of Λ type three-level atom which located at the defect position in the defect photonic crystal.[23] In the presence of the driving field and defect mode, the nature of quantum interference was depended on the initial atomic coherence.[24] Jiang *et al.* studied the spontaneous emission of a four-level atom driven by the closed-loop fields in the anisotropic photonic crystal.[25] The spontaneous emission was controlled by the photonic band gap, the amplitude and phase of coherent driving field. Liu *et al.* studied the spontaneous emission spectrum of the M-type five-level atom driven by microwave field in photonic crystal, and observed spectral line displacement, spectral line enhancement and spectral line suppression in the spontaneous emission spectra.[26]

So far, the spontaneous emission of the atom coupled by the bichromatic field in photonic crystals has not been studied. For the bichromatic excitation of the atom, the main theoretical method is the harmonic expansion method, which can not obtain the analytical solution.[27] In this paper, we propose a new theoretical method to calculate the spontaneous emission properties of the Λ-type three-level atom coupled by the bichromatic field in the anisotropic double-band photonic crystal. The expression of spontaneous emission spectrum of the Λ-type three-level atom is derived. Then, the state wave functions of the atom are obtained in the dressed state representation. Finally, the influences of the initial state of the atom, the width of double-band photonic band gap, the Rabi frequency intensity and the detuning δ of bichromatic field on the spontaneous emission spectra are discussed, and the phenomena are explained in the dressed state representation.

2. Theoretical model

2.1. Model derivation

A Λ-type three-level atom is embedded in an anisotropic double-band photonic crystal. The three-level atom is composed of an upper level $|0\rangle$ and two lower levels $|1\rangle$, $|j\rangle$, as shown in Fig. 1. The transition $|1\rangle \leftrightarrow |j\rangle$ is forbidden, the transition $|0\rangle \leftrightarrow |1\rangle$ with the resonant frequency ω_{01} being driven by the bichromatic field, and the transition $|0\rangle \rightarrow |j\rangle$ with the resonant frequency ω_j is coupled with the anisotropic double-band photonic crystal.

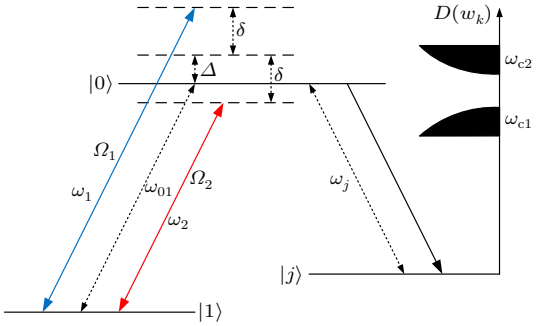


Fig. 1. The level structure of the Λ-type three-level atom.

The Rabi frequencies of bichromatic field are Ω_1 and Ω_2, and the frequencies of the bichromatic field are ω_1 and ω_2. The detunings between the two frequencies of the bichromatic field and the resonant frequency of the transition $|0\rangle \rightarrow |1\rangle$ are $\Delta_1 = \omega_1 - \omega_{01} = \Delta + \delta$, $\Delta_2 = \omega_2 - \omega_{01} = \Delta - \delta$, respectively, in which Δ is the detuning between the central frequency of the bichromatic field and the atomic resonant frequency ω_{01}. δ is the detuning between the two frequencies and the central frequency of the bichromatic field.

In the rotating wave approximation, the Hamiltonian and the atomic wave function in the interaction picture are written as

$$\hat{H} = \left(\hbar\Omega_1 \mathrm{e}^{-\mathrm{i}(\Delta+\delta)t} + \hbar\Omega_2 \mathrm{e}^{-\mathrm{i}(\Delta-\delta)t}\right)|0\rangle\langle 1| + \sum_k \hbar g_k \mathrm{e}^{-\mathrm{i}\delta_k t} b_k |0\rangle\langle j| + \mathrm{H.c.}, \tag{1}$$

$$|\Psi(t)\rangle = a_0(t)|0,0\rangle + a_1(t)|1,0\rangle + \sum_k a_j(t)|j,1_k\rangle, \tag{2}$$

where g_k is the coupling constant related to the transition frequency of atom $|0\rangle \rightarrow |j\rangle$, $\delta_k = \omega_k - \omega_j$ is the detuning between the emitted photon with ω_k and the transition $|0\rangle \rightarrow |j\rangle$ with ω_j. k is the k-th mode of the emitted field, $b_k^\dagger$ and b_k represent the creation and annihilation operators of the k-th vacuum mode with frequency ω_k.

Substituting the Hamiltonian (Eq. (1)) and state vector (Eq. (2)) into the Schrödinger equation $\hat{H}|\Psi(t)\rangle = \mathrm{i}\hbar\frac{\mathrm{d}}{\mathrm{d}t}|\Psi(t)\rangle$, we can derive the first-order differential equations for the amplitudes as follows:

$$\mathrm{i}\dot{a}_0(t) = \left(\Omega_1 \mathrm{e}^{-\mathrm{i}(\Delta+\delta)t} + \Omega_2 \mathrm{e}^{-\mathrm{i}(\Delta-\delta)t}\right)a_1(t) + \sum_k g_k \mathrm{e}^{-\mathrm{i}\delta_k t} a_j(t), \tag{3}$$

$$\mathrm{i}\dot{a}_1(t) = \left(\Omega_1^* \mathrm{e}^{\mathrm{i}(\Delta+\delta)t} + \Omega_2^* \mathrm{e}^{\mathrm{i}(\Delta-\delta)t}\right) a_0(t), \tag{4}$$

$$\mathrm{i}\dot{a}_j(t) = g_k^* \mathrm{e}^{\mathrm{i}\delta_k t} a_0(t). \tag{5}$$

Supposing $b_1(t) = a_1(t)\,\mathrm{e}^{-\mathrm{i}\Delta t}$, Eqs. (3) and (4) can be simplied as

$$\mathrm{i}\dot{a}_0(t) = \left(\Omega_1 \mathrm{e}^{-\mathrm{i}\delta t} + \Omega_2 \mathrm{e}^{\mathrm{i}\delta t}\right) b_1(t) + \sum_k g_k \mathrm{e}^{-\mathrm{i}\delta_k t} a_j(t), \tag{6}$$

$$\mathrm{i}\dot{b}_1(t) = \left(\Omega_1^* \mathrm{e}^{\mathrm{i}\delta t} + \Omega_2^* \mathrm{e}^{-\mathrm{i}\delta t}\right) a_0(t) + \Delta b_1(t). \tag{7}$$

Integrate Eq. (5)

$$a_j(t) = -\mathrm{i}g_k^* \int_0^t \mathrm{e}^{\mathrm{i}\delta_k t'} a_0(t')\,\mathrm{d}t'. \tag{8}$$

Substituting Eq. (8) into the last term of Eq. (6)

$$\sum_k g_k \mathrm{e}^{-\mathrm{i}\delta_k t} a_j(t) = -\mathrm{i}\int_0^t a_0(t') \sum_k g_k^2 \mathrm{e}^{-\mathrm{i}\delta_k (t-t')}\,\mathrm{d}t', \tag{9}$$

$G(t-t') = \sum_k g_k^2 \mathrm{e}^{-\mathrm{i}\delta_k (t-t')}$ is called delayed Green's function, and then Eq. (6) becomes

$$\begin{aligned}\mathrm{i}\dot{a}_0(t) = &\left(\Omega_1 \mathrm{e}^{-\mathrm{i}\delta t} + \Omega_2 \mathrm{e}^{\mathrm{i}\delta t}\right) b_1(t) \\ &-\mathrm{i}\int_0^t a_0(t') G(t-t')\,\mathrm{d}t'.\end{aligned} \tag{10}$$

In vacuum (Markov reservoir), according to the Weisskopf–Wigner theory, the dispersion relationship is $\omega_k = ck$, the corresponding density of states being $D(\omega_k) \approx 1$, the delayed Green's function being $G(t-t') = (\Gamma_0/2)\delta(t-t')$, and Γ_0 is the spontaneous relaxation rate, which is taken as 1 in the calculation. Then the last term of Eq. (10) can be changed as

$$\int_0^t a_0(t') G(t-t')\,\mathrm{d}t' = \frac{\Gamma_0}{2} a_0(t). \tag{11}$$

For the anisotropic double-band photonic crystal, the dispersion relationship is

$$\omega_k = \begin{cases} \omega_{\mathrm{c}2} + A_2 |k-k_0|^2, & |k| > |k_0|, \\ \omega_{\mathrm{c}1} - A_1 |k-k_0|^2, & |k| < |k_0|, \end{cases} \tag{12}$$

where $\omega_{\mathrm{c}1}$ and $\omega_{\mathrm{c}2}$ are the lower and upper edge frequencies of photonic crystal band gap, respectively. k_0 is the periodic structure constant of photonic crystal, $A_n \approx \omega_{\mathrm{c}n}/k_0^2$ $(n = 1, 2)$. The density of states and the delayed Green's function corresponding to this dispersion relation are

$$D(\omega_k) \approx \sqrt{\omega_k - \omega_{\mathrm{c}2}}\,\Theta(\omega_k - \omega_{\mathrm{c}2}) + \sqrt{\omega_{\mathrm{c}1} - \omega_k}\,\Theta(\omega_{\mathrm{c}1} - \omega_k), \tag{13}$$

$$G(t-t') = \frac{\alpha_{01}}{2}\left\{\frac{\mathrm{e}^{\mathrm{i}\left[\delta_{\mathrm{c}2}(t-t')+\pi/4\right]}}{\sqrt{4\pi(t-t')^3}} + \frac{\mathrm{e}^{\mathrm{i}\left[\delta_{\mathrm{c}1}(t-t')-\pi/4\right]}}{\sqrt{4\pi(t-t')^3}}\right\}, \tag{14}$$

where $\Theta(x)$ is the Heviside function. α_{01} is the coupling constant, $\alpha_{01} = 1$ being taken in the calculation and $\delta_{\mathrm{c}1} = \omega_j - \omega_{\mathrm{c}1}$, $\delta_{\mathrm{c}2} = \omega_j - \omega_{\mathrm{c}2}$.

From Eq. (14), we can obtain the Laplace transform of the Green function given by

$$\tilde{G}(s) = \frac{\alpha_{01}}{2}\left(\sqrt{\mathrm{i}s + \delta_{\mathrm{c}2}} - \mathrm{i}\sqrt{\mathrm{i}s + \delta_{\mathrm{c}1}}\right). \tag{15}$$

The Laplace transforms of Eqs. (7) and (10) can be written as

$$\begin{aligned}&\mathrm{i}\left[s\tilde{a}_0(s) - a_0(+0)\right] \\ &= \Omega_1 \tilde{b}_1(s + \mathrm{i}\delta) + \Omega_2 \tilde{b}_1(s - \mathrm{i}\delta) - \mathrm{i}\tilde{a}_0(s)\tilde{G}(s),\end{aligned} \tag{16}$$

$$\begin{aligned}&\mathrm{i}\left[s\tilde{b}_1(s) - b_1(+0)\right] \\ &= \Omega_1^* \tilde{a}_0(s - \mathrm{i}\delta) + \Omega_2^* \tilde{a}_0(s + \mathrm{i}\delta) + \Delta\tilde{b}_1(s).\end{aligned} \tag{17}$$

Suppose $s = s_n = -\mathrm{i}\delta_k + \mathrm{i}n\delta$, $n = 0, \pm1, \pm2, \ldots$, and bring it into Eqs. (16) and (17), respectively. Then an equation set composed of infinite equations can be obtained as

$$\begin{aligned}
&\mathrm{i}\left[s_0\tilde{a}_0(s_0) - a_0(+0)\right] = \Omega_1\tilde{b}_1(s_1) + \Omega_2\tilde{b}_1(s_{-1}) \\
&\qquad - \mathrm{i}\tilde{a}_0(s_0)\tilde{G}(s_0), \\
&\mathrm{i}\left[s_0\tilde{b}_1(s_0) - b_1(+0)\right] = \Omega_1^*\tilde{a}_0(s_{-1}) + \Omega_2^*\tilde{a}_0(s_1) + \Delta\tilde{b}_1(s_0), \\
&\mathrm{i}\left[s_1\tilde{a}_0(s_1) - a_1(+0)\right] = \Omega_1\tilde{b}_1(s_2) + \Omega_2\tilde{b}_1(s_0) \\
&\qquad - \mathrm{i}\tilde{a}_0(s_1)\tilde{G}(s_1), \\
&\mathrm{i}\left[s_1\tilde{b}_1(s_1) - b_1(+0)\right] = \Omega_1^*\tilde{a}_0(s_0) + \Omega_2^*\tilde{a}_0(s_2) + \Delta\tilde{b}_1(s_1), \\
&\mathrm{i}\left[s_{-1}\tilde{a}_0(s_{-1}) - a_0(+0)\right] = \Omega_1\tilde{b}_1(s_0) + \Omega_2\tilde{b}_1(s_{-2}) \\
&\qquad - \mathrm{i}\tilde{a}_0(s_{-1})\tilde{G}(s_{-1}), \\
&\mathrm{i}\left[s_{-1}\tilde{b}_1(s_{-1}) - b_1(+0)\right] = \Omega_1^*\tilde{a}_0(s_{-2}) + \Omega_2^*\tilde{a}_0(s_0) \\
&\qquad + \Delta\tilde{b}_1(s_{-1}), \\
&\quad\vdots \\
&\mathrm{i}\left[s_{\pm n}\tilde{a}_0(s_{\pm n}) - a_0(+0)\right] = \Omega_1\tilde{b}_1(s_{\pm n+1}) + \Omega_2\tilde{b}_1(s_{\pm n-1}) \\
&\qquad - \mathrm{i}\tilde{a}_0(s_{\pm n})\tilde{G}(s_{\pm n}), \\
&\mathrm{i}\left[s_{\pm n}\tilde{b}_1(s_{\pm n}) - b_1(+0)\right] = \Omega_1^*\tilde{a}_0(s_{\pm n-1}) + \Omega_2^*\tilde{a}_0(s_{\pm n+1}) \\
&\qquad + \Delta\tilde{b}_1(s_{\pm n}).
\end{aligned} \tag{18}$$

Ignoring the higher-order terms $\tilde{a}_0(s_{n+1})$, $\tilde{a}_0(s_{-n-1})$, $\tilde{b}_1(s_{n+1})$, $\tilde{b}_1(s_{-n-1})$ of the system of equations, $\tilde{a}_0(\mathrm{i}\delta_k)$ can be solved.

With Laplace transform, the Eq. (5) can be changed as

$$s\tilde{a}_j(s) - a_j(0) = -\mathrm{i}g_k\tilde{a}_0(\mathrm{i}\delta_k). \tag{19}$$

Based on the final value theorem $\lim\limits_{t\to+\infty} a_j(t) = \lim\limits_{s\to0} s\tilde{a}_j(s)$, we can get

$$a_j(t\to\infty) = -\mathrm{i}g_k\tilde{a}_0(\mathrm{i}\delta_k). \tag{20}$$

Then the spontaneous emission spectra of the atom can be expressed as

$$S(\delta_k) = D(\omega_k)\left|\frac{a_j(t\to\infty)}{g_k}\right|^2 = D(\omega_k)\left|\tilde{a}_0(\mathrm{i}\delta_k)\right|^2. \tag{21}$$

2.2. Dressed state

With the semi-classical method,[28] we can get the state wave function of the atom modified by the bichromatic field in the case of $\Delta = 0$, $\Omega_1 = \Omega_2 = \Omega$ as follows:

$$\begin{aligned}|\Psi(t)\rangle = & \mathrm{e}^{-\mathrm{i}\omega_1 t}\left[\alpha\sum_{n=-\infty}^{+\infty}J_n\left(\frac{\Omega}{\delta}\right)\mathrm{e}^{\mathrm{i}n\delta t}\right.\\ & \left.+\beta\sum_{n=-\infty}^{+\infty}J_n\left(-\frac{\Omega}{\delta}\right)\mathrm{e}^{\mathrm{i}n\delta t}\right]|1\rangle\\ & +\mathrm{e}^{-\mathrm{i}\omega_0 t}\left[-\alpha\sum_{n=-\infty}^{+\infty}J_n\left(\frac{\Omega}{\delta}\right)\mathrm{e}^{\mathrm{i}n\delta t}\right.\\ & \left.+\beta\sum_{n=-\infty}^{+\infty}J_n\left(-\frac{\Omega}{\delta}\right)\mathrm{e}^{\mathrm{i}n\delta t}\right]|0\rangle, \qquad (22)\end{aligned}$$

where $J_n(x)$ is the Bessel function and $\alpha = [a_1(0) - a_0(0)]/2$, $\beta = [a_1(0) + a_0(0)]/2$.

According to the state wave function, the energy spectrum of the atom driven by the bichromatic field is composed of a series of ladder decorated states $|\Phi\rangle_m^N$, $|\Phi\rangle_m^{N+1}$, with the resonant transition frequency between $|\Phi\rangle_m^N$ and $|\Phi\rangle_m^{N+1}$ ω_{01}, where $m = 0, \pm1, \pm2, \ldots, N$ is the total photon number of the bichromatic field. The dressed energy level structure is shown in Fig. 2.

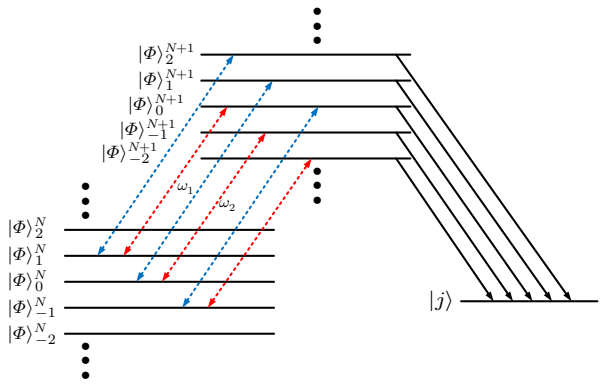


Fig. 2. Dressed states of a Λ-type three-level atom interacting with a bichromatic field.

The wave function of the dressed state can be expressed as

$$\begin{aligned}|\Phi\rangle_m^{N+1} = & \sum_{l=0,\pm1,\ldots}J_{2l+1-m}\left(-\frac{\Omega}{\delta}\right)\left|1,\frac{N}{2}+l+1,\frac{N}{2}-l\right\rangle\\ & +\sum_{l=0,\pm1\cdots}J_{2l-m}\left(-\frac{\Omega}{\delta}\right)\left|0,\frac{N}{2}+l,\frac{N}{2}-l\right\rangle, \qquad (23)\end{aligned}$$

$$\begin{aligned}|\Phi\rangle_m^N = & \sum_{l=0,\pm1,\cdots}J_{2l-m}\left(-\frac{\Omega}{\delta}\right)|1,N+l,N-l\rangle\\ & +\sum_{l=0,\pm1,\cdots}J_{2l+1-m}\left(-\frac{\Omega}{\delta}\right)|0,N+l,N-l-1\rangle. \qquad (24)\end{aligned}$$

The corresponding energy is

$$\varepsilon_m^{N+1} = (N+1)\hbar\omega_{01} + m\hbar\delta, \qquad (25)$$

$$\varepsilon_m^N = N\hbar\omega_{01} + m\hbar\delta, \qquad (26)$$

where $|n, N_1, N_2\rangle$, N_1, N_2 are the number of photons generated by the bichromatic field.

According to the Eqs. (22)–(24), the initial state of the atom can be expanded based on the energy levels $|\Phi\rangle_m^N$ and $|\Phi\rangle_m^{N+1}$. The initial probability of the atom on $|\Phi\rangle_m^N$ and $|\Phi\rangle_m^{N+1}$ at $t = 0$ can be calculated as

$$\rho_{mm}^{N+1} = {}_m^{N+1}\langle\Phi|\Psi(0)\rangle\langle\Psi(0)|\Phi\rangle_m^{N+1}, \qquad (27)$$

$$\rho_{mm}^{N} = {}_m^{N}\langle\Phi|\Psi(0)\rangle\langle\Psi(0)|\Phi\rangle_m^{N}. \qquad (28)$$

3. Numerical simulation and conclusion analysis

In this part, the spontaneous emission phenomena of Λ-type three-level atom driven by bichromatic field in anisotropic double-band photonic crystals and vacuum are investigated. The spontaneous emission spectra are plotted and analyzed with the different system parameters, such as the initial state of the atom, the position and width of photonic forbidden band gap, Rabi frequency intensity of the bichromatic field, the detuning between the two frequencies and the central frequency of the bichromatic field.

3.1. Influence of the initial state of the atom on the spontaneous emission spectra

In order to study the influence of the initial state of the atom, the spontaneous emission spectra of the atom in different initial states are plotted as shown in Fig. 3. Figures 3(a)–3(c) are the atomic spontaneous emission spectra in the vacuum reservoir. Figures 3(d)–3(f) are the atomic spontaneous emission spectra in the anisotropic double-band photonic.

As can be seen in Fig. 3, with the bichromatic excitation, the spontaneous emission spectrum of the atom exhibits a multi-peak comb-like structure and the emitted peaks are always located at $n\delta$, where $n = 0, \pm1, \pm2, \ldots$. When the initial state of the atom is $|1\rangle$, as shown in Figs. 3(a) and 3(d), the emitted peaks are located at $(2n+1)\delta$; when the initial state of the atom is $|0\rangle$, as shown in Figs. 3(b) and 3(e), the emitted peaks are located at $2n\delta$; when the initial state of the atom is $(1/\sqrt{2})|0\rangle + (1/\sqrt{2})|1\rangle$, as shown in Figs. 3(c) and 3(f), the emitted peaks appear at $n\delta$. When the emitted peaks are placed in the anisotropic photonic band gap as shown in Figs. 3(d)–3(f), it will be annihilated because of the forbidden effect of the anisotropic photonic band gap.

Next, we explain the above phenomena in the dressed-state representation. It is well known that a series of dressed states with equal energy intervals can be produced in the dressed-state representation, as shown in Fig. 2. The spontaneous emission peaks are generated by the $|\Phi\rangle_m^{N+1} \to |j\rangle$ transitions of the dressed state. The probability of the atomic initial population in the dressed state can be calculated according to the Eqs. (27) and (28). When the initial state of the atom is $|1\rangle$, the probability of the initial atomic population in

the dressed state $|\Phi\rangle^{N}_{\pm1,\pm3,\ldots}$ and $|\Phi\rangle^{N+1}_{0,\pm2,\pm4,\ldots}$ is 0. It means that there is no population in the energy levels of $|\Phi\rangle^{N}_{\pm1,\pm3,\ldots}$ and $|\Phi\rangle^{N+1}_{0,\pm2,\pm4,\ldots}$. Therefore, there only exists the transition of $|\Phi\rangle^{N+1}_{\pm1,\pm3,\ldots} \to |j\rangle$, and then the emitted peak only appears at $(2n+1)\,\delta$, as shown in Figs. 3(a) and 3(d). When the initial state of the atom is $|0\rangle$, the probability of the initial atomic population in the dressed state $|\Phi\rangle^{N}_{0,\pm2,\pm4,\ldots}$ and $|\Phi\rangle^{N+1}_{\pm1,\pm3,\ldots}$ is 0, which means that there is no population on the energy levels of $|\Phi\rangle^{N}_{0,\pm2,\pm4,\ldots}$ and $|\Phi\rangle^{N+1}_{\pm1,\pm3,\ldots}$. So there is only the transition $|\Phi\rangle^{N+1}_{0,\pm2,\pm4,\ldots} \to |j\rangle$, and the emitted peaks only appear at $2n\delta$, as shown in Figs. 3(b) and 3(e). When the initial state of the atom at $(1/\sqrt{2})\,|0\rangle + (1/\sqrt{2})\,|1\rangle$, the probability of the initial atomic population in the dressed state $|\Phi\rangle^{N}_{m}$ and $|\Phi\rangle^{N+1}_{m}$ is not 0, which means that the population is distributed in all dressed energy levels. The transitions from $|\Phi\rangle^{N+1}_{m}$ to $|j\rangle$ all exist, and the emitted peaks appear at $n\delta$, as shown in Figs. 3(c) and 3(f). In a word, choosing different initial states can control the position of the spontaneous emission peak, while adjusting the photonic band gap can annihilate the emitted peak at different positions.

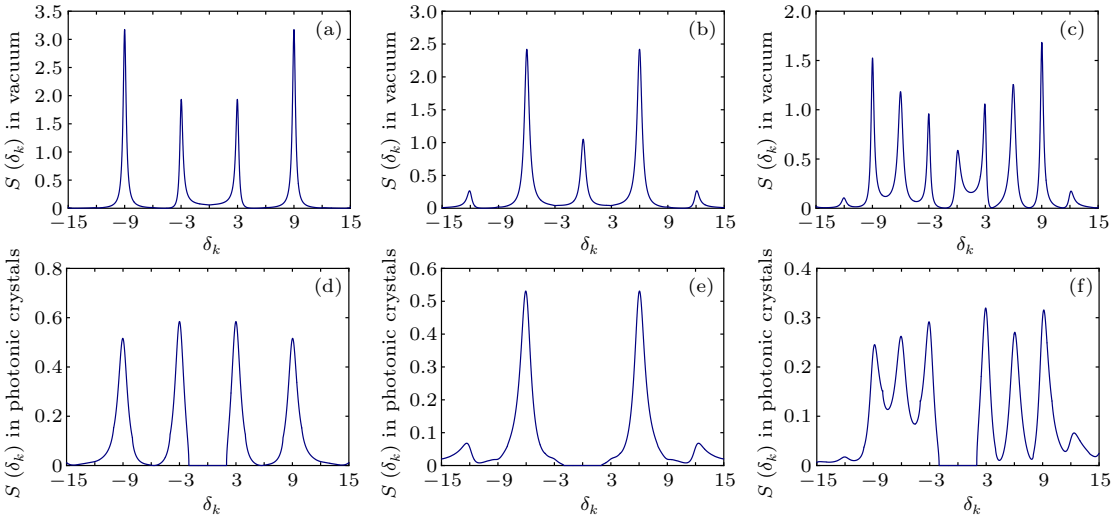


Fig. 3. Atomic spontaneous emission spectra in vacuum and anisotropic double-band photonic crystal. The others parameters are set as $\Delta = 0$, $\delta = 3$, $\Omega_1 = \Omega_2 = 4.8$, $\omega_j = 100$, $\omega_{c1} = 98$, $\omega_{c2} = 102$. In panels (a) and (d) $a_0 = 0$, $a_1 = 1$. In panels (b) and (e) $a_0 = 1$, $a_1 = 0$. In panels (c) and (f) $a_0 = 1/\sqrt{2}$, $a_1 = 1/\sqrt{2}$.

3.2. Influence of photonic crystal band gap on spontaneous emission spectra

In this section, the effects of the width of the photonic double-band gap on the spontaneous emission spectra are investigated. Spontaneous emission spectra of the atom in vacuum are firstly drawn as shown in Fig. 4(a), and then, the spontaneous emission spectra of the atom with different widths of the band gap in the photonic crystal are plotted as shown in Figs. 4(b)–4(d).

From Fig. 4(a), it can be seen that there are four emitted peaks located at $\delta_k = -6$, $\delta_k = -3$, $\delta_k = 0$, and $\delta_k = 3$ in the spontaneous emission spectra of the atom in vacuum. When the atomic resonant frequency is in the center of the double-band photonic gap with band gap edge frequencies $\omega_{c1} = 99$ and $\omega_{c2} = 101$ as shown in Fig. 4(b), the emitted peak at $\delta_k = 0$ is annihilated because of the forbidden effect of the photonic band gap, meanwhile the emitted peaks at $\delta_k = -3$ and $\delta_k = -6$ are close to each other and overlap, and the dark line disappears. When the width of the photonic band gap increases with the edge frequencies $\omega_{c1} = 98$ and $\omega_{c2} = 102$ as shown in Fig. 4(c), the emitted peak at $\delta_k = -3$ is significantly enhanced due to the singular density of states near the photonic crystal band edge. When the width of the photonic band gap increases again with the edge frequencies $\omega_{c1} = 97$ and $\omega_{c2} = 103$ as shown in Fig. 4(d), the emitted peak at $\delta_k = 3$ enters into the forbidden band gap and disappears, but the emitted peak at $\delta_k = -3$ is close to the photonic band edge and becomes stronger. Therefore, changing the width of the photonic band gap can enhance the spontaneous emission peaks near the band edge and annihilate the one in the forbidden gap.

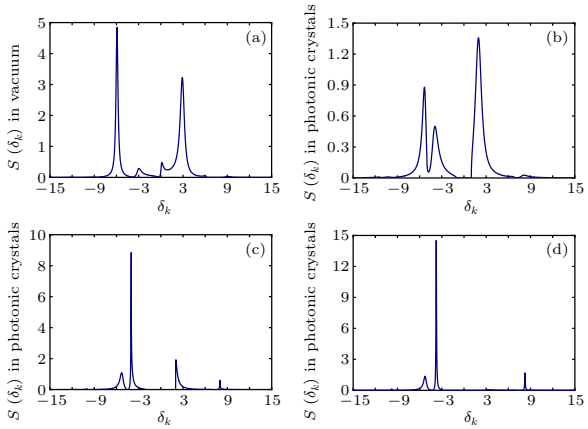


Fig. 4. Atomic spontaneous emission spectra in vacuum and photonic crystal. The others parameters are set as $a_0 = 0$, $a_1 = 1$, $\Delta = 0$, $\delta = 3$, $\Omega_1 = 1$, $\Omega_2 = 4$, $\omega_j = 100$; (a) in vaccum; (b) $\omega_{c1} = 99$, $\omega_{c2} = 101$; (c) $\omega_{c1} = 98$, $\omega_{c2} = 102$; (d) $\omega_{c1} = 97$, $\omega_{c2} = 103$.

3.3. Influence of Rabi frequency intensity of the bichromatic field on spontaneous emission spectra

The Rabi frequency intensity of the bichromatic field can also have a greater impact on the spontaneous emission spectra of the atom. The spontaneous emission spectra with different Rabi frequency intensities $\Omega_1 = \Omega_2 = 1.3$, 2, 3.3 are respectively plotted in vacuum and in anisotropic double-band photonic crystal as shown in Fig. 5.

When $\Omega_1 = \Omega_2 = 1.3$ in vacuum as shown in Fig. 5(a), a fluorescence quenching point appears at $\delta_k = 0$ due to quantum interference between the two transition channels which is generated on the condition that the molecular term in the radiation spectrum expression is zero.[29] When $\Omega_1 = \Omega_2 = 2$ as shown in Fig. 5(b), the two inner emitted peaks overlap and the quantum interference effect has not occurred between two transition channels. Therefore, the emitted peak at $\delta_k = 0$ is not zero. As can be seen in Figs. 5(a)–5(c), with the increasing intensity of Rabi frequency of the bichromatic field in vacuum, the inner peaks gradually decrease and the outside peaks gradually increase. It can be explained in the dressed state picture. The population distribution on each dressed energy level is different with different Rabi frequency intensities of bichromatic field, which can result in different emitted peak intensities. According to the analysis in Subsection 3.1, when the initial state of the atom is $|1\rangle$, the initial population can only distribute on the levels $|\Phi\rangle^N_{0,\pm2,\pm4,\ldots}$ and $|\Phi\rangle^{N+1}_{\pm1,\pm3,\ldots}$. From Eq. (26), it can be considered that the population at the initial time all locates at $|\Phi\rangle^N_0$. There are only two transition channels between $|\Phi\rangle^N_{0,\pm2,\pm4,\ldots}$ and $|\Phi\rangle^{N+1}_{\pm1,\pm3,\ldots}$: $|\Phi\rangle^N_0 \to |\Phi\rangle^{N+1}_1 \to |\Phi\rangle^N_2 \to |\Phi\rangle^{N+1}_3, \ldots$ and $|\Phi\rangle^N_0 \to |\Phi\rangle^{N+1}_{-1} \to |\Phi\rangle^N_{-2} \to |\Phi\rangle^{N+1}_{-3}, \ldots$ When the intensity of the Rabi frequency is small, the population is distributed on $|\Phi\rangle^{N+1}_{\pm1}$ through the transition $|\Phi\rangle^N_0 \to |\Phi\rangle^{N+1}_{\pm1}$, and then a strong emitted peak is formed at $\delta_k = \pm2$. When the Rabi frequency intensity increases, the population gradually transfers to $|\Phi\rangle^{N+1}_{\pm3}$ through the transition $|\Phi\rangle^{N+1}_{\pm1} \to |\Phi\rangle^N_{\pm2} \to |\Phi\rangle^{N+1}_{\pm3}$. The emitted peak at $\delta_k = \pm2$ becomes weaker, and the emitted peak at $\delta_k = \pm6$ gets stronger as shown in Figs. 5(a)–5(c). However, when the atom is embedded in the anisotropic double-band photonic crystal as shown in Figs. 5(d)–5(f), the spontaneous emission spectra are significantly different from that in vacuum. It can be found that the emission peaks are significantly enhanced when the Rabi frequency intensity of the bichromatic field is small as shown in Fig. 5(d), and the emission peaks decrease rapidly with the increasing of the Rabi frequency intensity as shown in Figs. 5(e) and 5(f). This phenomenon is caused by the combined effect of the photonic band gap and the bichromatic field. Therefore, adjusting the Rabi frequency can control the intensity of different radiation peaks, and the photonic crystal can significantly enhance the outside emitted peaks.

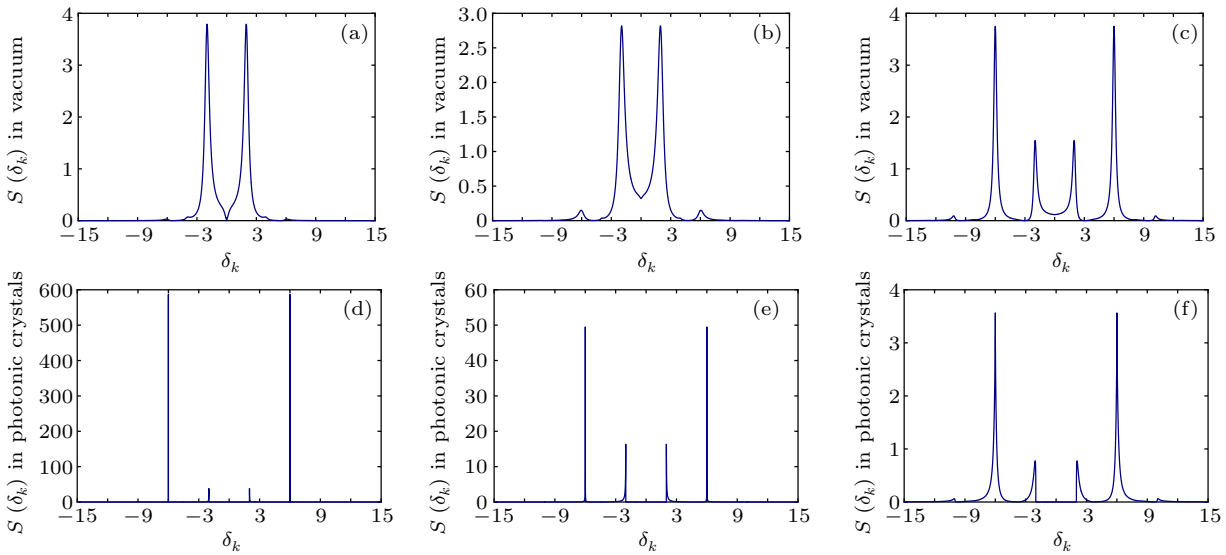


Fig. 5. Atomic spontaneous emission spectrum in vacuum and photonic crystal. The others parameters are set as $a_0 = 0$, $a_1 = 1$, $\Delta = 0$, $\delta = 2$, $\omega_{c1} = 98$, $\omega_{c2} = 102$, $\omega_j = 100$. In panels (a) and (d) $\Omega_1 = \Omega_2 = 1.3$. In panels (b) and (e) $\Omega_1 = \Omega_2 = 2$. In panels (c) and (f) $\Omega_1 = \Omega_2 = 3.3$.

3.4. Influence of the ratio Ω/δ between Rabi frequency intensity and the detuning of the bichromatic field on spontaneous emission spectra

In the previous section, we find that the intensity of the Rabi frequency of the bichromatic field can affect the properties of the spontaneous emission spectra. From Eq. (22), we can see that the Bessel function is independent of the ratio Ω/δ between Rabi frequency intensity and the detuning of the bichromatic field. So in this section, the effects of the ratio Ω/δ on the spontaneous emission spectra are studied. The spontaneous emission spectra with different ratios Ω/δ are respectively plotted in vacuum and in anisotropic double-band photonic crystal as shown in Fig. 6.

Comparing Figs. 6(a) and 6(c), Figs. 5(b) and 6(b) in vac-

uum, we can observe that when the ratio Ω/δ is same, the shape of the radiation spectrum is similar and the intensity of the spontaneous emission peak is same. But the interval of the closed emitted peaks are 2δ as discussed in Subsection 3.1. In addition, as the ratio Ω/δ increases, the intensity of the outside emitted peak becomes higher. From Figs. 6(a) and 6(b), it can be seen that when the Rabi frequency intensity is the same, the increase of the detuning δ reduces the emitted peak on the outside. It can be explained in the dressed state picture as follows. Based on Eqs. (23) and (24), the expression of the dressed level contains a Bessel function, which is independent of the ratio Ω/δ. Therefore, the height of the emitted peak depends on the ratio Ω/δ. When the detuning δ increases but the Rabi frequencies are same, it can not enough to transfer the population to the following dressed levels through the two transition channels $|\Phi\rangle_0^N \to |\Phi\rangle_1^{N+1} \to |\Phi\rangle_2^N \to |\Phi\rangle_3^{N+1}, \ldots$ and $|\Phi\rangle_0^N \to |\Phi\rangle_{-1}^{N+1} \to |\Phi\rangle_{-2}^N \to |\Phi\rangle_{-3}^{N+1}, \ldots$ When the Rabi frequency is increased, as shown in Fig. 6(c), the height of the radiation peak can be restored to the same height as that in Fig. 6(a). However, when the atom is embedded in the anisotropic double-band photonic crystal, the interval of the spontaneous emission peaks is still related to the detuning δ, as shown in Figs. 6(d)–6(f). As the detuning δ increases, the distance between the emitted peaks becomes larger. Different from the case of vacuum, the shape of the emitted peak is not only determined by the ratio Ω/δ, but also modulated by the photonic band gap. When the ratio Ω/δ increases but the detuning δ is small in the anisotropic double-band photonic crystal as shown in Figs. 5(e) and 6(d), the emitted peaks get closer to the band edge and become much stronger, which attributes to the modulation effect of the photonic band gap. When the ratio Ω/δ and the detuning δ both increase in the anisotropic double-band photonic crystal as shown in Figs. 6(e) and 6(f), the interval between the adjacent emitted peak and the band edge becomes farther. There is no enhancement in the spontaneous emission spectra and the shape of the spontaneous emission spectra is the same as the situation in vacuum as shown in Figs. 6(b) and 6(c). The difference is that the height of the emitted peak outside the photonic band gap decreases rapidly and the emitted peak inside the photonic band gap is annihilated.

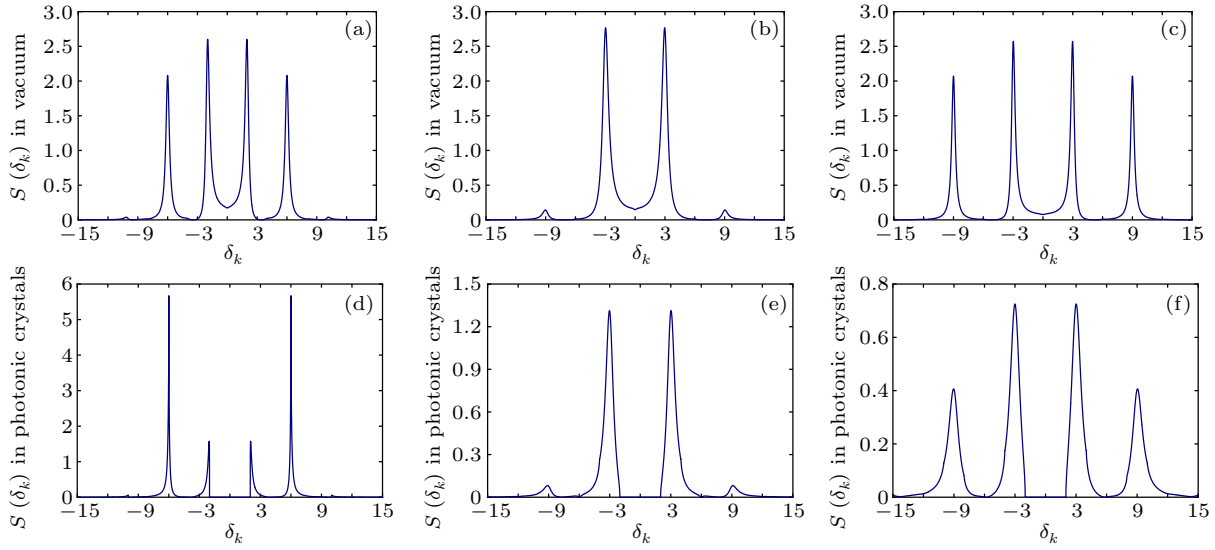


Fig. 6. Atomic spontaneous emission spectrum in vacuum and photonic crystal. The others parameters are set as $a_0 = 0$, $a_1 = 1$, $\Delta = 0$, $\omega_{c1} = 98$, $\omega_{c2} = 102$, $\omega_j = 100$. In panels (a) and (d) $\Omega_1 = \Omega_2 = 3$, $\delta = 2$. In panels (b) and (e) $\Omega_1 = \Omega_2 = 3$, $\delta = 3$. In panels (c) and (f) $\Omega_1 = \Omega_2 = 4.5$, $\delta = 3$.

3.5. Influence of atomic resonant transition frequency on spontaneous emission spectra

When the resonant transition frequency ω_j of the atomic transition $|0\rangle \to |j\rangle$ coupled with the anisotropic double-band photonic crystal are different, the atomic spontaneous emission spectra are plotted as shown in Fig. 7.

From Fig. 7, it can be seen that when the atomic resonant transition frequency is outside the lower edge frequency of the photonic band gap, the emitted peak at $\delta_k = -3$ on the left side is enhanced and the emitted peak at $\delta_k = 3$ is annihilated. When the atomic resonant transition frequency is within the photonic band gap as shown in Fig. 7(b), the emitted peak on the left side is weakened by the photonic band gap and a dark line caused by the quantum destructive interference appears in the spontaneous emission spectra. When the atomic resonant transition frequency is outside the upper edge frequency of the photonic band gap as shown in Fig. 7(c), one of the two emitted peaks on the left side enters the band gap and is annihilated, and the other also decreases. The emitted peak on the right side in the emitted spectra is far away from the photonic band gap, so the emitted peak does not change.

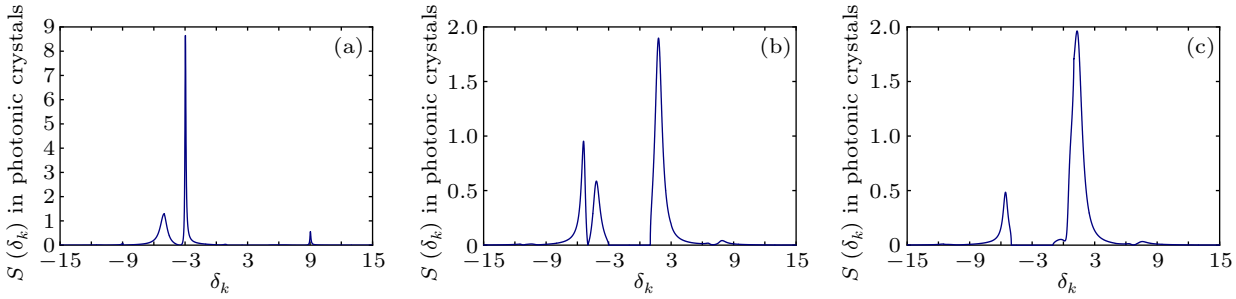


Fig. 7. Atomic spontaneous emission spectrum in photonic crystal. The others parameters are set as $a_0 = 0$, $a_1 = 1$, $\Delta = 0$, $\delta = 3$, $\Omega_1 = 1$, $\Omega_2 = 4$, $\omega_{c1} = 98$, $\omega_{c2} = 102$. (a) $\omega_j = 97$, (b) $\omega_j = 101$, (c) $\omega_j = 103$.

4. Conclusion

With n-times iteration method, the spontaneous emission spectra of the Λ-type three-level atom coupled by the bichromatic field in the anisotropic double-band photonic crystal are studied. The spontaneous emission of the atom strongly depends on the initial state of the atom, the Rabi frequency intensity and the detuning δ of the bichromatic field. With the bichromatic excitation, the multi-peak comb-shaped peaks in the spontaneous emission spectra of the atom are determined by the dressed state $|\Phi\rangle_m^{N+1} \to |j\rangle$. The detuning δ of the bichromatic field determines the interval of the adjacent emitted peak. When the initial state of the atom is at the lower level, the emitted peaks locate at $(2n+1)\,\delta$. When the initial state of the atom is at the upper level, the emitted peaks locate at $2n\delta$. The enhancement occurs when the emitted peak locates near the photonic band edge. The annihilation occurs when the emitted peak locates inside the photonic band gap. The Rabi frequency intensity Ω of the bichromatic field can change the population distribution on the dressed level $|\Phi\rangle_m^{N+1}$. The heights of the emitted peaks can remain unchanged when the ratio Ω/δ is a constant. Modulated by both the bichromatic field and the photonic crystal band gap, there happens fluorescence enhancement and fluorescence quenching in the emission spectra. Spontaneous emission enhancement has potential applications in bioimaging, novel photonic devices, and improving the sensitivity of biosensing techniques. The research content of this paper provides a certain theoretical basis for controlling the atomic spontaneous emission.

Acknowledgment

Project supported by the Natural Science Foundation of Jilin Province of China (Grant No. 20220101031JC).

References

[1] Kamaha J S D, Talla M J H, Noubissie S, Fotsin H B and Woafo P 2022 *Opt. Quantum Electron.* **54** 1
[2] Zeinab K, Saeed G and Mohammad M 2016 *Quantum Inform. Proc.* **15** 199
[3] Chen J Y, Song F, Ma Y C, Wang Z P and Yu B L 2017 *Laser Phys. Lett.* **14** 095201
[4] Chen J Y, Song F, Wang Z P and Yu B L 2018 *Laser Phys. Lett.* **15** 65205
[5] Fleischhauer M, Matsko A B and Scully M O 2000 *Phys. Rev. A* **62** 013808
[6] Ottaviani C, Vitali D, Artoni M, Cataliotti F and Tombesi P 2003 *Phys. Rev. Lett.* **90** 197902
[7] Seke J and Herfort W N 1988 *Phys. Rev. A* **38** 833
[8] Mollow B R 1969 *Phys. Rev.* **188** 1969
[9] Zhu S Y, Narducci L M and Scully M O 1995 *Phys. Rev. A* **52** 4791
[10] Hu L, Hu X M and Hu Q M 2021 *Chin. Phys. B* **30** 64211
[11] Ding C L, Li J H and Yang X X 2010 *Opt. Commun.* **283** 2705
[12] Qi T, Huo X X, Zhang J and Liu X S 2020 *Chin. Phys. B* **29** 053201
[13] Zhang H F, Yuan J P, Wang L R, Xiao L T and Jia S T 2021 *Chin. Phys. B* **30** 053202
[14] Hu X M, Xu Q, Li J Y, Li X X, Shi W X and Zhang X 2006 *Opt. Commun.* **260** 196
[15] Hu X M, Shi W X, Xu Q, Guo H J, Li J Y and Li X X 2006 *Phys. Lett. A* **352** 543
[16] Jin K, Xie X T and Jiang Z Y 2013 *Chin. Phys. B* **22** 014205
[17] Zhang L Q, Zhu C X, Yu S C, Zhou Z R and Ge D H 2021 *Results Phys.* **31** 105054
[18] Yang Y P, Fleischhauer M and Zhu S Y 2003 *Phys. Rev. A* **68** 043805
[19] Zhou R L, Peng J C, Li H J, Zhang G M and Lin F 2003 *Spectrosc. Spect. Anal.* **23** 657
[20] Zhang S Q, Li H, Li M X, Liu X H and Song L J 2020 *Int. J. Theor. Phys.* **59** 2880
[21] Huang X S, Liu H L and Dong W 2012 *Chin. Phys. B* **21** 054218
[22] Zhang K, Zhu Y P, Jiang L and Zhang H Z 2010 *Chin. Phys. B* **19** 054206
[23] Roshan E S 2012 *Commun. Theor. Phys.* **57** 115
[24] Roshan E S 2013 *J. Mod. Opt.* **60** 713
[25] Jiang L, Wan R G and Yao Z H 2016 *Chin. Phys. B* **25** 104204
[26] Liu R G 2014 *Int. J. Theor. Phys.* **53** 4351
[27] Peng L, Nakajima T and Ning X 2006 *Phys. Rev. A* **74** 043408
[28] Kim H, Park J R and Lee H 2000 *J. Phys. B: At, Mol. Opt. Phys.* **33** 1703
[29] Wu J H, Li A J, Ding Y, Zhao Y C and Gao J Y 2005 *Phys. Rev. A* **72** 023802